Automated Sleep-Spindle Detection in Healthy Children Polysomnograms

Leonardo Causa*, Claudio M. Held, *Senior Member, IEEE*, Javier Causa, Pablo A. Estévez, *Senior Member, IEEE*, Claudio A. Perez, *Senior Member, IEEE*, Rodrigo Chamorro, Marcelo Garrido, Cecilia Algarín, and Patricio Peirano

***Abstract*—We present a new methodology to detect and characterize sleep spindles (SSs), based on the nonlinear algorithms, empirical-mode decomposition, and Hilbert–Huang transform, which provide adequate temporal and frequency resolutions in the electroencephalographic analysis. In addition, the application of fuzzy logic allows to emulate expert's procedures. Additionally, we built a database of 56 all-night polysomnographic recordings from children for training and testing, which is among the largest annotated databases published on the subject. The database was split into training (27 recordings), validation (10 recordings), and testing (19 recordings) datasets. The SS events were marked by sleep experts using visual inspection, and these marks were used as golden standard. The overall SS detection performance on the testing dataset of continuous all-night sleep recordings was 88.2% sensitivity, 89.7% specificity, and 11.9% false-positive (FP) rate. Considering only non-REM sleep stage 2, the results showed 92.2% sensitivity, 90.1% specificity, and 8.9% FP rate. In general, our system presents enhanced results when compared with most systems found in the literature, thus improving SS detection precision significantly without the need of hypnogram information.**

***Index Terms*—EEG, empirical-mode decomposition (EMD), Hilbert–Huang transform (HHT), sleep-pattern recognition, sleep spindles (SSs).**

I. Introduction

THE CYCLIC alternance between sleep and waking is one of the most prominent and profound rhythms in life. Although sleep can be perceived as rest, it is actually also a period of substantial neurological and physiological activity. Indeed, neurons in most parts of the brain remain active during sleep, and the brain consumes a significant amount of energy with this neural activity. It is easily conceivable that neurons are responsible for autonomic functions, such as respiration remain active in both sleep and waking, but neurons in other brain areas also remain active, often, in a highly synchronous and rhythmic manner [1].

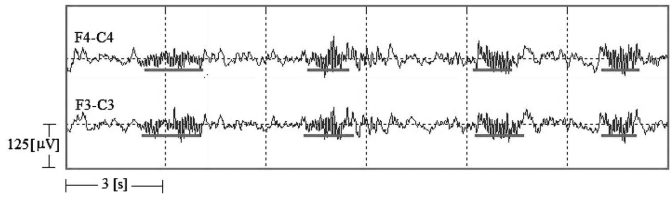

Fig. 1. SSs marked by a sleep expert in an EEG recording. The length of the horizontal line indicates the duration of an event. Figure shows two frontocentral EEG derivations (F4-C4 and F3-C3) during NREMS-2.

Sleep is not a homogeneous process. Two different states are described: REM sleep (REMS) and non-REM sleep (NREMS) [2], [3], which are electroencephalographically, physiologically, and behaviorally distinct from one another.These sleep states are identified by the temporal concordance among relevant EEG, electrooculographic (EOG), and electromyographic (EMG) patterns. NREMS is further subdivided into four stages, numbered from 1 to 4, indicating the depth of sleep and the presence of specific EEG patterns [3]. Currently, NREMS stages 3 and 4 are pooled together and termed slow wave sleep (SWS) [4]–[6].

Although the functions of sleep remain largely unknown, one of the most exciting hypotheses is that sleep contributes importantly to processes of memory and brain plasticity [7]–[10]. Currently, NREMS stages have become a major focus of attention.

Sleep-pattern identification allows for adequate classification of sleep–wake states and stages, but the patterns are also interesting by themselves. In particular, sleep spindles (SSs) are one of the most characteristic EEG patterns during sleep and a hallmark of the onset of NREMS-2. They are defined as discrete bursts of 10–16 Hz waves with a typical duration of 0.5–2 s, usually mounted on slower waves with larger amplitudes (see Fig. 1) [3]–[6].

SS patterns have been proposed to be a marker of normal brain functional development and integrity, and deviations from normal patterns suggest altered brain functioning or a pathology [11]. Further, SS have been suggested to provide necessary conditions for plastic modification underlying memory formation [12]–[14]. In line with this, NREMS-2 with SS as a central feature has been proposed as a possible candidate for *offline memory processing* with several groups demonstrating: 1) SS

Manuscript received January 23, 2010; revised March 30, 2010, and May 10, 2010; accepted May 14, 2010. Date of publication June 14, 2010; date of current version August 18, 2010. This work was supported in part by the Chilean Science and Technology Funding Agency, Chile, under Grant Fondo Nacional de Desarrollo Científico y Tecnológico 1070668, in part by the National Institutes of Health under Grant HD 33487, and in part by the Electrical Engineering Department and the Instituto de Nutrición y Tecnología de los Alimentos, Universidad de Chile. *Asterisk indicates corresponding author*.

*L. Causa is with the Department of Electrical Engineering, Universidad de Chile, Santiago, Chile (e-mail: lcausa@ing.uchile.cl).

C. M. Held is with the Department of Electrical Engineering, Universidad de Chile, Santiago, Chile, and also with Apacomint Ltda, Santiago 190, Chile (e-mail: cheld@apacom.cl).

J. Causa is with the Department of Electrical Engineering, Universidad de Chile, Santiago, Chile (e-mail: jcausa@ing.uchile.cl).

P. A. Estévez and C. A. Perez are with the Department of Electrical Engineering and the Advanced Mining Technology Center, Universidad de Chile, Santiago, Chile (e-mail: pestevez@ing.uchile.cl; clperez@ing.uchile.cl).

R. Chamorro, M. Garrido, C. Algarín, and P. Peirano are with the Sleep Laboratory, Instituto de Nutrición y Tecnología de los Alimentos, Universidad de Chile, Santiago, Chile (e-mail: rchamorro@inta.cl; mgarrido@inta.cl; calgarin@inta.cl; ppeirano@inta.cl).

Digital Object Identifier 10.1109/TBME.2010.2052924

increase following successful learning; 2) overnight memory-improvement relation to the amount of NREMS-2 and SS activity; and 3) relationships between SS and general measures of learning aptitude [15]–[18]. Furthermore, recent results bring additional support for the existence of distinct slow and fast SS, with potentially different functional significance; in particular, fast SS being involved in processing sensorimotor and mnemonic information [15], [19]–[21]. Research to date, however, continues to be fragmentary and has been conducted almost exclusively in adults. Although sleep-state organization in early infancy and especially NREMS have been related to individual outcomes in measures of cognitive functions and attention in later childhood and early adolescence [22], the relationships between SS and learning in childhood have received little attention.

Visual detection of SS in polysomnograms by sleep experts is an intensive, time-consuming task, and introduces specialist-associated biases [23], [24]. Automated detection is a powerful tool to standardize detection and reduce expert time devoted to this task. Hence, there is a need to develop an automated, reliable SS detector tool.

Different research groups have been working on automated SS detection. Bódizs *et al.* [25] used bandpass filtering on segments of EEG recordings of 12 subjects (total duration: about 3–4 h) to detect SS events. They adjusted the filters according to amplitude and frequency criteria to identify slow and fast SS. Their results showed 92.9% sensitivity and 58.4% false-positive (FP) rate.

Huupponen *et al.* [26] compared four different methods to detect bilateral SS in healthy adult subjects: method 1 used a bilateral sigma index based on the fast-Fourier transform (FFT) spectrum complemented with SS amplitude analysis based on an filter-impulse-response (FIR) filter, method 2 used only a bilateral sigma index, method 3 was based on fuzzy detectors, and method 4 used a fixed SS amplitude detector. Tests applied on 12 all-night recordings (approximately 96 h total, with 6043 bilateral SS events marked by experts) showed that all methods provided the best results on the NREMS-2 parts of the recordings. Method 1 presented 70% sensitivity and 98.6% specificity, with an FP rate of 32% in NREMS-2. The other methods showed decreasing performances, and method 4 showing the poorest results. In a previous work [27], the same group described an adaptive module to determine the optimal amplitude threshold to detect SS events on six all-night recordings: two were used as training set (TS) (approximately 15 h) and four were used as testing set (approximately 30 h). This module was further developed and used in [26]. They reported an overall performance in the testing set (3335 SS events marked by experts) of 79% sensitivity and 3.4% FP rate.

Estévez *et al.* [28] used short-time Fourier transform (SFT), feature extraction, and merge neural gas in segments of two nap sleep recordings: one was used for training (about 45 min), and the other was used as testing dataset (about 45 min) to detect SS events in infants. Their results showed 62.9% sensitivity for the testing dataset. Ventouras *et al.* [29] published a feasibility study of applying a multilayer perceptron (MLP) architecture to detect SS events on a single recording using bandpass-filtered EEG. The sensitivity of the network ranged from 79.2% to 87.5%, the specificity ranged from 88.4% to 97.3%, and the FP rate ranged from 3.8% to 15.5%. Gorur *et al.* [30] used SFT on the EEG for feature extraction and MLP and support vector machines (SVMs) for SS detection only in segments of recordings classified as NREMS-2 (5 h 45 min). For testing MLP, 1142 equally distributed samples of SS and non-SS were used, thus showing 88.7% sensitivity. To test the SVM system, 175 equally distributed samples of SS and non-SS were applied, and showed 95.4% sensitivity.

Schönwald *et al.* [31] applied matching pursuit (MP) on amplitude, frequency, and duration characteristics to define the optimal amplitude threshold to detect SS events in nine recordings in a sample of NREMS-2, SWS, and REMS. The results showed 80.6% sensitivity and specificity in NREMS-2, and 81.2% sensitivity and specificity for all stages together. Zygierewicz *et al.* [32] applied MP to detect SS events in ten NREMS-2 recordings of healthy adult subjects, reaching 90% sensitivity.

Held *et al.* [33] used bandpass-filtered EEG on the sigma band, amplitude thresholds, and duration criteria. The method was applied on a testing set consisting of two continuous nap sleep recordings of infants (totaling 6 h with a total of 803 SS events marked by the sleep experts). Results showed 87.7% sensitivity and 8.1% FP rate. Schimicek *et al.* [34] detected SS events from recordings of ten subjects using EEG filtering, amplitude and duration criteria, and artifact treatment; the method performance showed 89.7% sensitivity and 6.5% FP rate.

This paper has two main objectives. The first is to present a new methodology to detect and characterize SS based on nonlinear algorithms: empirical-mode decomposition (EMD) [35], [36], Hilbert–Huang transform (HHT) [36], and fuzzy logic. These methodologies significantly improve SS detection precision. In particular, the use of EMD and HHT provide better temporal and frequency resolutions in the EEG analysis, and the application of fuzzy logic allows to emulate expert's procedure in SS detection. The second objective is to generate a significant annotated database of all-night polysomnographic recordings of children (56 recordings) to train and test this and other methods.

II. Methodology

A. Subjects and Recordings

We studied all-night polysomnographic recordings of 56 healthy ten-year-old children. The research protocol was approved by the Institutional Review Boards of the University of Michigan Medical Center, Ann Arbor, MI, USA; the ethical committee of the Instituto de Nutrición y Tecnología de los Alimentos (INTA), Universidad de Chile, Chile; by the Office of Protection from Research Risk, National Institutes of Health (NIH), USA; and by the Chilean Science and Technology Funding Agency (CONICYT), Chile. Parental signed informed consent and child assent were obtained.

1) Procedures: One-night recordings were performed in the Sleep Laboratory at INTA, in a special quiet and comfortable

room during the children's spontaneous night sleep. The procedures were standardized to limit the potential influences of environment, circadian rhythms, and/or food intake on sleep–wake patterns and other related physiological variables. Children and their mothers were transported from home to the laboratory; they arrived at least one hour before their usual dinner time. Upon arrival, mother and child had the opportunity to become familiar with personnel and setting, while playing or relaxing. Then, they ate dinner together and engaged in their own routines before the child's bedtime. The mothers also stayed in the laboratory overnight, sleeping in a nearby room after the child fell asleep. The room temperature was maintained constant (20–22°C) throughout the recording session.

The recordings were performed with an Easy EEG-II 32-channel polygraph (Cadwell, WA, USA, 2000) including: EEG signals with electrode placement according to the international 10-20 system [37], rapid eye movements monitored by EOG, tonic chin and diaphragmatic EMG using surface electrodes, motor activity of both upper and lower limbs recorded independently by piezoelectric crystal transducers and EMG of the right and left tibialis anterior muscles, abdominal respiratory movements using a mercury strain gauge, airflows by a nasal cannula and a mouth thermistor, electrocardiogram using surface electrodes, skin temperature, and oxymetry were also recorded. Child behavior was observed directly and noted throughout.

All data were converted online from analog to digital signals; each channel was sampled at a rate of 200 Hz, collected on a hard drive, and then, transformed to European data format (EDF) [38] for offline analyses.

To detect SS, we used both frontocentral EEG derivations (F4-C4 and F3-C3) because the sigma activity is predominant in these derivations, whereas the posterior EEG derivations are the primary reference for background activity [39]–[43].

2) Database and SS Visual Scoring: Independent scorers of the INTA Sleep Laboratory visually analyzed all recordings and marked the beginning and the end of the SS events using the visualization and marking tools of the *sleep analyzer*. *Sleep analyzer* is a sleep recordings analysis system based on MATLAB, which includes different tools to visualize, mark, filter, process, and analyze polysomnographic signals, sleep patterns, and hypnograms. This tool was developed by the Biomedical Engineering Laboratory of the Electrical Engineering Department, in collaboration with the Sleep Laboratory, INTA, both from the Universidad de Chile.

The recordings were divided into three different sets. Neural networks [44]–[47] were applied to group the recordings to obtain an adequate distribution of all sleep states and stages in each set, resulting in a TS of 27 recordings (216 h approximately, 48 669 SS), a validation set (VS) of ten recordings (80 h approximately, 22 443 SS), and a testing set of 19 recordings (152 h approximately, 40 412 SS).

B. SSs Detection System

The proposed SS detection system can be described as an analysis cascade of four modules, as shown in Fig. 2. In Module 1, the two frontocentral EEG derivations are processed to define EEG zones where to search for SS candidates. Module 2 is applied on the defined EEG zones to generate first-step SS candidates (SSc1). Module 3 validates SSc1 based on SS features, by reducing the number of wrong detections and generating second-step SS candidates (SSc2). Module 4 further refines the analysis to generate the final SS detection (start and end positions).

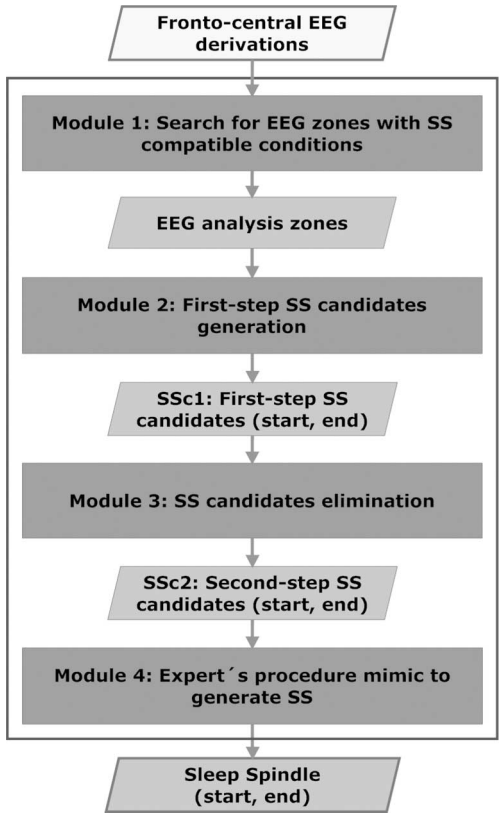

Fig. 2. Block diagram of the proposed SS detection system. The inputs are the frontocentral EEG derivations. Modules 1 and 2 are candidate generation processes, whereas Modules 3 and 4 are elimination processes. The system outputs are the starting and ending positions of each SS event detected.

The system parameters were adjusted using the TS to establish adequate thresholds and fine-tuned applying the VS. Traditionally, the amplitude thresholds have been selected using training recording or by some spindles scoring criteria, but there is not a single definition [27]. Our research group defined the accepted amplitude range values between 15 and 120 μV, considering that higher values would correspond to artifacts. Similarly, there is not a single definition about the frequency band allowed for SS, for example, some authors use bands as wide as 10–16 Hz [27], whereas others constrain it to 11–15 Hz [48] or 12–15 Hz [49]. In this paper, we use the same definition that was used in [27] to define the sigma band.

1) Module 1 (Detection of EEG Analysis Zones): Module 1 searches for EEG zones compatible with SS presence, i.e., NREMS-2 and SWS [3]–[6]. The purpose of this is to reduce the search zones of SS candidates, since EMD–HHT (Module 2) are computer-intensive tasks.

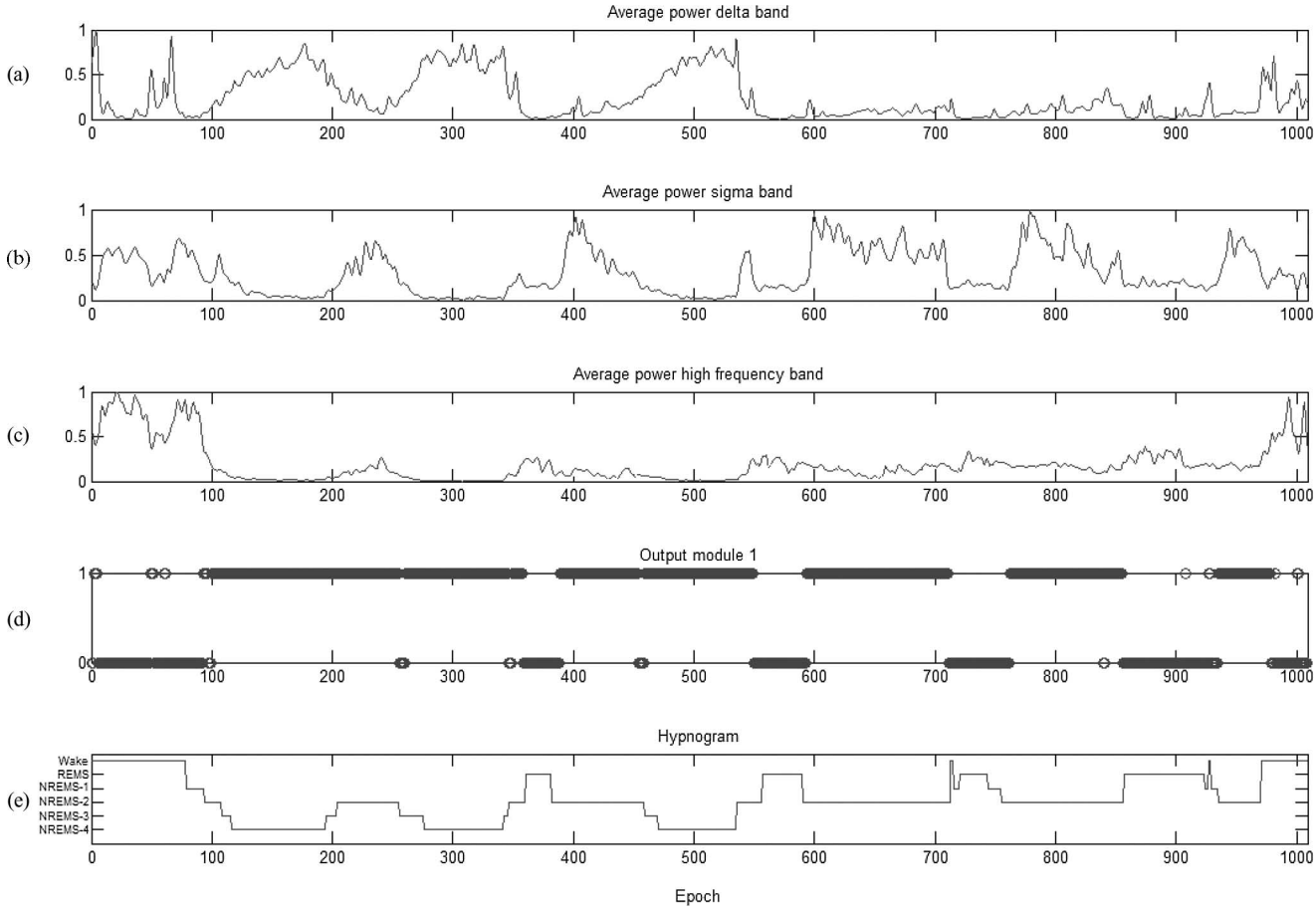

Fig. 3. Example of the Module 1 process in an all-night sleep recording. FFT is applied on each frontocentral EEG derivation, obtaining the AP for the: (a) delta band ([0.5, 3] Hz), (b) sigma band ([10, 16] Hz), and (c) high frequency band ([30, 60] Hz). (d) Result of Module 1, i.e., the EEG zones where to focus the SS detection. "1" indicates that the EEG zone is compatible with the presence of SS, otherwise it is "0." (e) Corresponding hypnogram (referential information, the hypnogram is not a part of the process). It can be seen that Module 1 successfully selects NREMS-2 and SWS epochs.

FFT is applied on each frontocentral EEG derivation on a moving Hamming window of 2.56 s (512 samples) with an overlap of 1.28 s (256 samples) between windows. Then, the power of bands delta ([0.5, 3] Hz), sigma ([10, 16] Hz), and *high frequency* ([30, 60] Hz) are calculated. The power of the *physiological* band ([0.5, 60] Hz) is also calculated to normalize the previous indexes. The average power (AP) for 30-s EEG windows is obtained for each band: AP_D (delta band), AP_S (sigma band), and $\mathrm{AP}_{\mathrm{HF}}$ (high-frequency band), throughout the whole EEG recording. The duration of the EEG windows was empirically determined using the TS. Each window is qualified as an EEG analysis zone if either AP_D or AP_S is above a certain threshold, and at the same time, $\mathrm{AP}_{\mathrm{HF}}$ is below another threshold, according to the following rules:

$$1)\ \text{if}\ (\mathrm{AP}_{Dn} \geq \alpha_1 \wedge \mathrm{AP}_{\mathrm{HF}n} \leq \alpha_3) \Rightarrow \mathrm{EEG\,zone}(n) = 1;$$

$$2)\ \text{if}\ (AP_{Sn} \geq \alpha_2 \wedge \mathrm{AP}_{\mathrm{HF}n} \leq \alpha_3) \Rightarrow \mathrm{EEG\,zone}(n) = 1;$$

$$3)\ \text{else}\ \mathrm{EEG\,zone}(n) = 0.$$

Parameters α_1 and α_2 are threshold values to discriminate the EEG zones with significant power in the delta and sigma bands, respectively (interest zones); α_3 is meant to discard the EEG zones with high noise levels. The threshold values were empirically obtained using the TS. The epochs classified as NREMS-2 typically show a high AP_S, epochs classified as SWS show a high AP_D, and epochs classified as wakefulness show a high $\mathrm{AP}_{\mathrm{HF}}$. Fig. 3 shows an example of the EEG power analysis and the results of Module 1. Compared to the hypnogram of the same data, Module 1 successfully separates the zones of interest.

2) Module 2 (SSs Candidate Generation (SSc1)): Module 2 is applied only to the zones defined by Module 1 to generate SSc1. It can be divided into three stages. In stage 1, EMD, FFT, and HHT are applied to obtain the instantaneous amplitude $(a_{\mathrm{IMF}(i)}(t))$ and instantaneous frequency $(\omega_{\mathrm{IMF}(i)}(t))$ of the frontocentral EEG derivations, where a is in microvolts and ω is in Hertz. Both $a_{\mathrm{IMF}(i)}(t)$ and $\omega_{\mathrm{IMF}(i)}(t)$ must meet certain criteria simultaneously to qualify an SS candidate, which are applied by means of fuzzy logic in stage 2. Stage 3 applies duration criteria.

a) Stage 1 (EMD–FFT–HHT): The nature of the EEG data and the SS characteristics make it inadequate to apply detection methods based only in FFT, amplitude, and duration criteria. Therefore, we use EMD and HHT to generate SS candidates, because they allow a better resolution in the time and

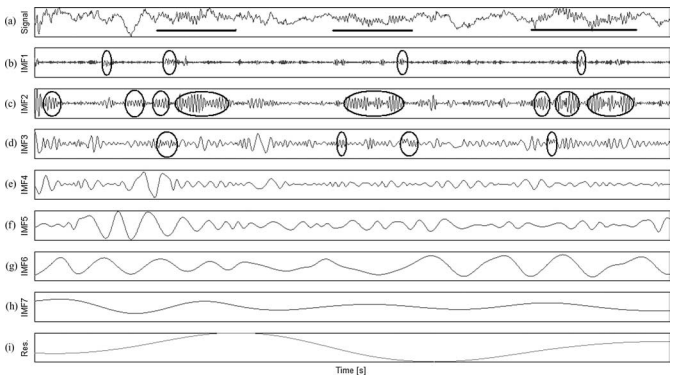

Fig. 4. Example of the application of EMD to a NREMS-2 EEG signal. (a) Original signal showing three SS events marked by the sleep expert. (b)–(h) EMD IMFs 1 to 7. (i) Residue of the EMD. Only the first three IMFs show events related to SS (circles); the rest involve slower frequencies. In this case, IMF2 shows the highest power level in the sigma band; hence, it is the primary IMF. IMF1 and IMF3 correspond to secondary IMFs.

frequency domains [50]. Other applications have shown that EMD–HHT can be a powerful technique for biomedical signal analysis [51]–[53], and particularly, for neural data analysis [50].

EMD is a signal decomposition method that operates in an iterative form. It decomposes the signal in a set of components called *intrinsic-mode functions* (IMFs). Each includes components of similar frequencies only. In each iteration, the EMD separates the signal in a high-frequency component (IMF) and a lower frequencies component (residue). The first iteration creates IMF1; the second iteration creates IMF2 by applying EMD to residue 1 and obtaining a residue 2. The EMD is completed once the residue is close to a flat zero signal [35]. HHT [36] is a technique that allows the representation of a signal in the frequency and time domains simultaneously.

EMD is applied to the zones of EEG derivations defined by Module 1. Then, HHT is used to obtain the $a_{\mathrm{IMF}(i)}(t)$ and $\omega_{\mathrm{IMF}(i)}(t)$ for the first three IMFs. Extensive trials with the TS showed that analyzing the first three IMFs of the EEG signals was enough to capture SS, because they only carried significant power information about the sigma band (see Fig. 4). The power level in the sigma band varies among these three components depending on the EEG characteristics; therefore, FFT is applied to establish the IMF with the highest power in the sigma band in each window, which we call as the primary IMF (IMF_P), according to the following equation:

$$\mathrm{IMF}_P = \max(P_{(\mathrm{SS})\mathrm{IMF}1}, P_{(\mathrm{SS})\mathrm{IMF}2}, P_{(\mathrm{SS})\mathrm{IMF}3}) \quad (1)$$

where $P_{(\mathrm{SS})\mathrm{IMF}i}$ is the sigma band power for IMF i ($i = 1$, 2, or 3). The others IMFs are referred to as secondary IMF (IMF_{Sj}). The secondary IMFs are eliminated from further analysis if their sigma power is below a certain threshold, according to the following equation:

$$\mathrm{IMF}_{Sj} = \begin{cases} \mathrm{IMF}_i, & P_{(\mathrm{SS})\mathrm{IMF}\,i} \geq \beta_1 \\ 0, & \text{otherwise} \end{cases} \quad (2)$$

where $j = 1$ or 2, $i = 1$, 2, or 3, and $i \neq P$. The parameter β_1 was obtained empirically using the TS.

HHT is applied to the primary IMF and the surviving secondary IMFs, obtaining the corresponding $a_{\mathrm{IMF}(i)}(t)$ and $\omega_{\mathrm{IMF}(i)}(t)$.

b) Stage 2 (Fuzzy Criteria): In Section II-B, we defined the initial amplitude and frequency range values, which have variations among different authors.This fact and trials with the TS determined the application of fuzzy-logic criteria on $a_{\mathrm{IMF}(i)}(t)$ and $\omega_{\mathrm{IMF}(i)}(t)$ to determine the instantaneous fuzzy amplitude ($fa_{\mathrm{IMF}(i)}(t)$) and the instantaneous fuzzy frequency ($f\omega_{\mathrm{IMF}(i)}(t)$). The thresholds of the maximum and minimum values for amplitude and frequency for an SS event were fuzzified as follows:

$$fa_{\mathrm{IMF}(i)} = \{0/10, 1/15, 1/120, 0/150\} \quad (3)$$

$$f\omega_{\mathrm{IMF}(i)} = \{0/9.5, 1/10, 1/16, 0/16.5\} \quad (4)$$

and are applied to IMF_P and IMF_{Sj}. In the aforementioned expressions, the four terms between the brackets are the points defining each trapezoid. The *numerator* is the value of the membership function at the corresponding value of the variable, which is indicated by the *denominator*.

Once the fuzzy values are obtained, the instantaneous product ($PI_{\mathrm{IMF}(i)}(t)$) is used to ensure simultaneous compliance to both amplitude and frequency, by combining $fa_{\mathrm{IMF}(i)}(t)$ and $f\omega_{I\mathrm{MF}(i)}(t)$

$$PI_{\mathrm{IMF}i}(t) = fa_{\mathrm{IMF}(i)}(t) f\omega_{\mathrm{IMF}(i)}(t). \quad (5)$$

Then, the maximum instantaneous product ($PI_{\max}(t)$) is obtained among the $PI_{\mathrm{IMF}(i)}(t)$ obtained for IMF_P and IMF_{Sj} as follows:

$$PI_{\max}(t) = \max(PI_{\mathrm{IMF}P}(t), PI_{\mathrm{IMF}S1}(t), PI_{\mathrm{IMF}S2}(t)). \quad (6)$$

$PI_{\max}(t)$ indicates the presence of an SS candidate, if it surpasses a threshold of 0.5, as determined with the TS.

c) Stage 3 (Duration Criteria): SS are trains of waves. Therefore, consecutive $PI_{\max}$ (outputs of stage 2) above the threshold will be first-step SSc1 if certain duration criteria are met. Consecutive samples are grouped together, forming pulses. To overcome noise corruption, pulses less than 0.2 s apart are joined together and their duration expanded from the beginning of the first pulse until the end of the last pulse. These trains of pulses are the outputs of Module 2, as shown by the example in Fig. 5.

3) Module 3 [SSs Candidate Elimination (SSc2)]: The purpose of Module 3 is to reduce the number of FP detections without losing true-positive (TP) detections, discriminating according to some SSc1 features. This module uses morphological and frequency information to filter and validate SSc1.

The EEG segments containing SSc1 are preprocessed using an FIR passband filter, with cutoff frequencies of [0.5; 25] Hz to eliminate artifacts and noise. Then, three consecutive peaks (min–max–min or max–min–max) are established by three consecutive sign changes in the slope of the signal, which

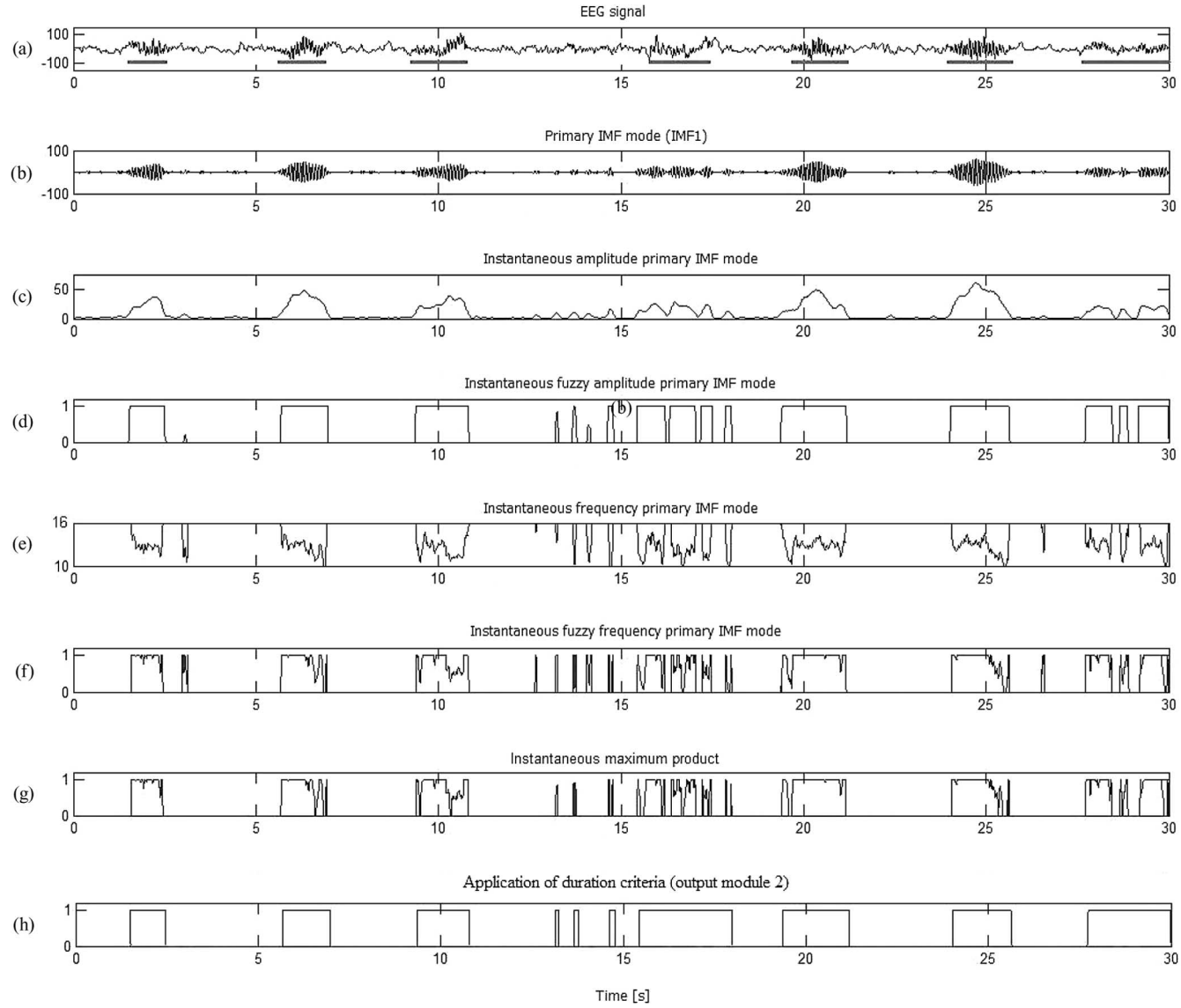

Fig. 5. Example of Module 2, stages 1, 2, and 3. (a) EEG signal segment with seven SS marked by the sleep expert. (b) Primary IMF (in this case IMF1) obtained by applying EMD. The secondary IMFs did not meet the minimum energy requirement and were discarded. (c) Instantaneous amplitude $a_{\mathrm{IMF}(1)}(t)$ obtained by applying HHT to IMF_P. (d) Instantaneous fuzzy amplitude $fa_{\mathrm{IMF}(1)}(t)$. (e) Instantaneous frequency $w_{\mathrm{IMF}(1)}(t)$ obtained by applying HHT. (f) Instantaneous fuzzy frequency $fw_{\mathrm{IMF}(1)}(t)$. (g) Instantaneous maximum product, $PI_{\max}(t)$. (h) First-step SSc1. Note the correlation between Module 2 output in (h) and the SS events marked by the sleep expert in (a).

are determined using linear regression. Three simple features are calculated: amplitude, frequency, and symmetry. Then, the average and standard deviation for each feature are calculated in each SSc1. Empirical threshold values are applied on these features to eliminate and generate the SSc2. Fig. 6 shows examples of features distribution extracted from SSc1 of the TS. The graphs combine average and standard deviation for frequency and amplitude, according to SS events (TP) and non-SS events (FP) marked by the sleep experts. SS events tend to show average values within a characteristic SS range and smaller standard deviation values.

4) Module 4 (Expert's Procedure Mimicking): Usually, SS are mounted on slower waves with larger amplitudes, which causes problems because these waves may interrupt and mask the SS trains. In manual analysis of the recording, the sleep expert does a visual recognition of the SS candidate to determine if it is a really SS or only sigma band activity, which does not satisfy the morphological and duration criteria for SS. Module 4 mimics the expert's procedure based on duration criteria and context analysis to generate the final SS detection (start and end positions).

SSc2 less than 0.25 s apart are grouped together and their duration expanded from the beginning of the first component until the end of the last component. The *amplitude* of each surviving train is obtained as the weighted average of all merged trains amplitudes. Trains lasting less than 0.1 s are eliminated. Then, trains less than 0.5 s apart are added together using the same process.

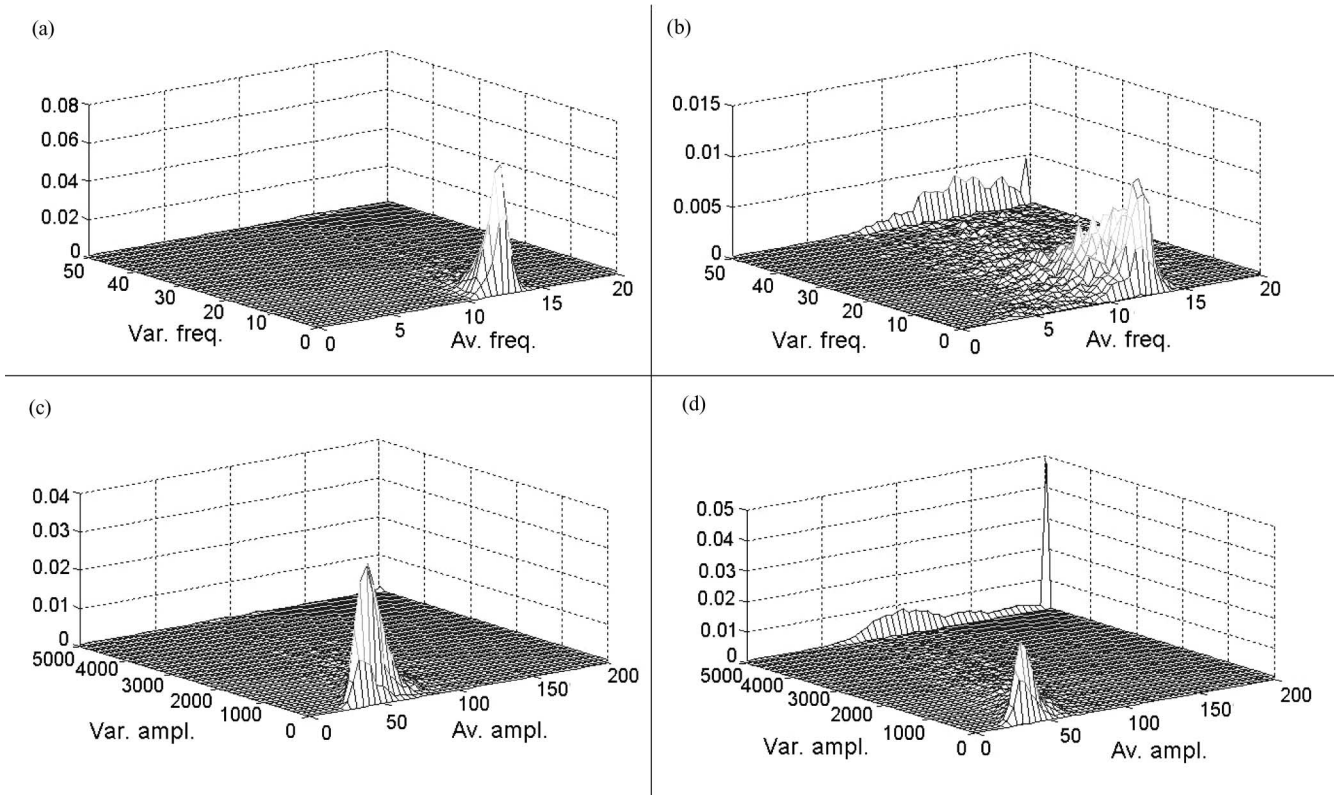

Fig. 6. Examples of average and standard deviation distribution of SSc1 features of the training dataset. (a) Frequency for SS events (TP). (b) Same for non-SS events (FP). (c) Amplitude for SS events (TP). (d) Same for non-SS events (FP). True SS events show average values in characteristic ranges and smaller standard deviation values.

Finally, we use the AP in the sigma and delta bands (computed in Module 1) to define rules of elimination according to the train durations:

$$1)\ \text{if } \mathrm{AP}_{Dn} \geq \delta_1$$
$$\Rightarrow \text{trains lasting less than } 0.4\,\text{s are eliminated;}$$
$$2)\ \text{else if } \mathrm{AP}_{Sn} \geq \delta_2$$
$$\Rightarrow \text{trains lasting less than } 0.3\,\text{s are eliminated;}$$
$$3)\ \text{else, trains lasting less than } 0.5\,\text{s are eliminated;}$$

where AP_{Dn} is the AP in the delta band, AP_{Sn} is the AP in the sigma band, and *n* is the corresponding 30-s EEG window containing SSc2. δ_1 and δ_2 were adjusted using the TS.

III. Experimental Results

The system was trained and the parameters were adjusted by means of an iterative process using the TS and VS, the latter being used to prevent over adjustment. The process begun with the selection of a set of parameters (P_1) within the normally accepted SS ranges. The model with parameters P_1 was evaluated on the TS and VS, obtaining the model errors $(\mathrm{FP/TP})_{\mathrm{TS}}$ and $(\mathrm{FP/TP})_{\mathrm{VS}}$. In the next iteration, a different set of parameters (P_2) was built: based on the $\mathrm{FP}_{\mathrm{TS}}$ and $\mathrm{FN}_{\mathrm{TS}}$ results, the parameter values were changed, aiming at reducing $(\mathrm{FP/TP})_{\mathrm{TS}}$. Once P_2 was determined, $(\mathrm{FP/TP})_{\mathrm{VS}}$ was measured. The parameter set P_3 was chosen as the set with smallest $(\mathrm{FP/TP})_{\mathrm{VS}}$ between P_1 and P_2. Then, P_4 was created using the same procedure as P_2, and P_5 was obtained as the set with smallest $(\mathrm{FP/TP})_{\mathrm{VS}}$ between P_3 and P_4. The iteration process continued until no further decrease in $(\mathrm{FP/TP})_{\mathrm{TS}}$ was found, or until an increase in $(\mathrm{FP/TP})_{\mathrm{VS}}$ was detected. The final model (P_f) was then applied to the untouched testing dataset, which did not participate in the adjustment process, to measure the performance of the system.

We used a quite strict criterion to determine system-expert agreement. If an SS marked by the system did not coincide at least in 75% with one established by an expert, it was labeled as FP. On the other hand, if an SS marked by the system was longer by 0.5 s or more than the established by the expert, the exceeding portion was marked as FP. The criteria used in other publications are not explicit. To characterize the true negative (TN), the sleep experts defined non-SS events as EEG data with sigma band activity, but not fulfilling morphology conditions for SS in visual inspection.

The overall results for each dataset for continuous all-night sleep recordings using the final model (optimal set of thresholds) are presented in Table I. Table II shows the results for the testing dataset in NREMS-2 and SWS. These are better in NREMS-2 than in SWS.

IV. Analysis of Results

The automated system detected most of the SS events. Results for the testing dataset in continuous EEG recordings show that 35 663 SS events were correctly identified by the automated

TABLE I
SS DETECTION RESULTS ON EACH DATASET

Set	SS events		Expert-system agreement in SS events (TP)	Expert-system agreement in non-SS events (TN)	Marked, but not detected (FN)	Detected, but not marked (FP)	Sensitivity [%]	Specificity [%]	False-positive rate [%]
	Marked by expert	Automated detection							
Training	48669	49346	43872	47956	4797	5474	90.1	89.8	11.1
Validation	22443	23197	20397	22765	2046	2800	90.9	89.0	12.1
Testing	40412	40487	35663	42128	4749	4824	88.2	89.7	11.9

Notes: Sensitivity = TP/(TP + FN), Specificity = TN/(TN + FP), and FP rate = FP/(TP + FP).

TABLE II
DETECTION RESULTS IN NREMS-2 AND SWS ON THE TESTING DATASET

Stages	SS events		Expert-system agreement in SS events (TP)	Expert-system agreement in non-SS events (TN)	Marked, but not detected (FN)	Detected, but not marked (FP)	Sensitivity [%]	Specificity [%]	False-positive rate [%]
	Marked by expert	Automated detection							
NREMS-2	27480	27791	25324	22431	2156	2467	92.2	90.1	8.9
SWS	12932	12696	10339	19697	2593	2357	79.9	89.3	18.6

system with an overall performance of 88.2% sensitivity, 89.7% specificity, and 11.9% of FP rate (see Table I). On the other hand, the global results for the TS, VS, and testing dataset present a low rate of dispersion, thus indicating an adequate distribution of the recordings among each dataset (see Table I).

The best results in the testing dataset were obtained in NREMS-2 with 92.2% sensitivity, 90.1% specificity, and an FP rate of 8.9% (see Table II). Detection results in SWS were poorer, apparently due to the high levels of delta activity, which introduces ambiguity on the SS identification. The system can spot sigma activity included in the signal because of its bandpass filters that eliminate the delta effects, generating FP detections.

The SS detection described can be divided in two steps; first is a candidate's generation process (Modules 1 and 2) and the second is a candidate's elimination process (Modules 3 and 4). Hence, it is very important that the first step detects all or most SS events, whereas the second step should eliminate most FPs, losing as few as possible TPs. The outputs of the modules show the evolution of the detection process: the increasing precision has the cost of losing some TP detections. In Fig. 7, this evolution on the testing dataset is shown as a ROC curve, which presents the sensitivity as a function of the FP rate. At the output of Module 2, about of 99% of the SS events are detected, but with a high FP rate of 88.9%. Module 3 is an intermediate step that introduces a significant improvement in the FP rate: it reduces the TP to FP rate from about 1:9 to about 1:1, at a cost of about 6.5% of TP. Finally, Module 4 detects 88.2% of the SS events, with an FP rate of 11.9%. The modules outputs show a similar detection performance when comparing all-night [see Fig. 7(a)] and NREMS-2 [see Fig. 7(b)] recordings.

It is suitable to compare results of different SS detection systems in the same way, since there is a tradeoff between the sensitivity and the FP rate. As mentioned earlier, Fig. 7 shows the ROC curves of our system. Other points in the graphs correspond to the results of other automated SS detection systems published in the literature (only comparable works). Our system matches or outperforms other published results, as it can be seen that

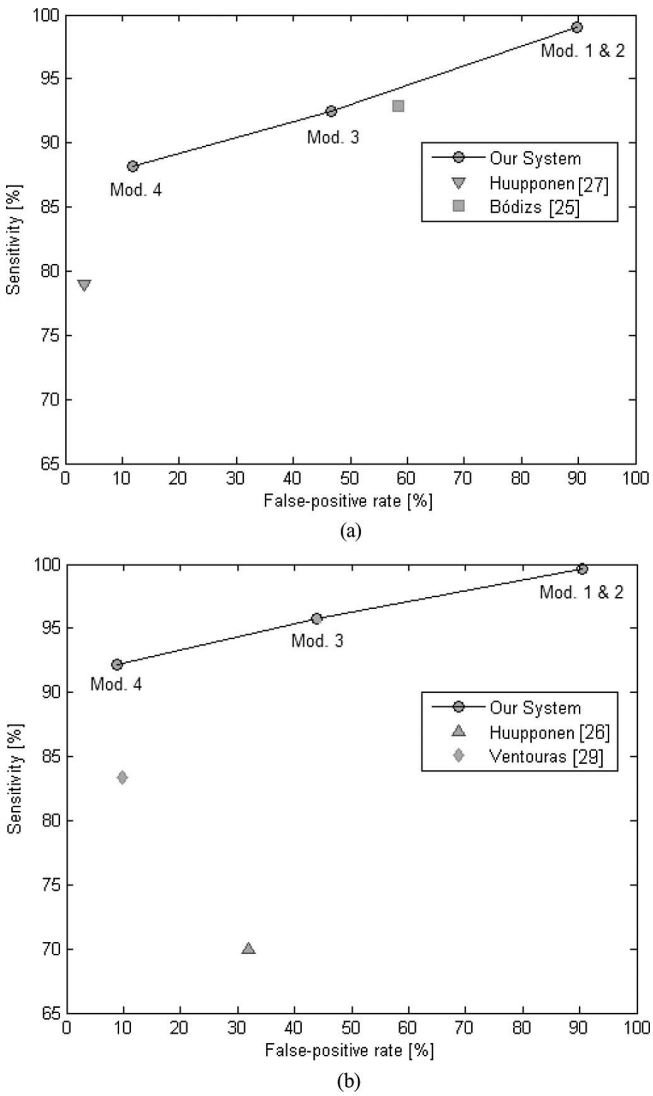

Fig. 7. ROC curves of the proposed SS detection system (Modules 1, 2, 3, and 4) compared to others published in the literature. The output of the system corresponds to Module 4, but intermediate results are available as well. (a) ROC curve for continuous all-night recordings. (b) ROC curve for NREMS-2 only.

TABLE III
COMPARISON OF DIFFERENT PUBLISHED AUTOMATED SS DETECTION SYSTEMS: RESULTS FOR COMPLETE AND MIXED SEGMENTS OF EEG RECORDINGS

Ref.[a]	Authors[b]	SS detection			Total recordings[d]	Subjects[e]	Data sets[f]	Sample Universe[g]	Methodology[h]
		Sensitivity[c] [%]	Specificity[c] [%]	False-positive rate[c] [%]					
	This work	88.2	89.7	11.9	56	Children	Training: 26 rec. Validation: 10 rec. Testing: 19 rec.	Complete all-night sleep recording. 40,412 SS events on testing set	EMD-HHT, FFT, fuzzy logic, features extraction and expert's procedure
[27]	Huuponen et al. (2000)	79.0	NR	3.4	6	Adults	Training: 2 rec. Testing: 4 rec.	Complete all-night sleep recording. 3,335 SS events on testing data set	Amplitude analysis based in fuzzy detectors
[33]	Held et al. (2004)	87.7	NR	8.1	5	Infants	Training: 3 rec. Testing: 2 rec.	Complete nap sleep recording. 803 SS events on testing data set	Morphological criteria, fuzzy logic and expert's procedure
[25]	Bódizs et al. (2009)	92.9	NR	58.4	12	Adults	NR	EEG segments of recording in NREMS1-4. 2,140 SS events marked by experts	Band-pass filtered EEG adjusted using frequency and amplitude criteria
[28]	Estévez et al. (2007)	62.9	NR	NR	2	Infants	Training: 1 rec. Testing: 1 rec.	Segments of nap sleep recordings (all states and stages)	SFT, features extraction and merge neural-gas
[31]	Schönwald et al. (2006)	81.2	81.2	NR	9	Adults	Training and testing data sets are the same	EEG segments of recording. 725 SS events marked by experts	Amplitude and duration criteria and matching pursuit
[34]	Schimicek et al. (1994)	89.7	NR	6.5	10	Adults	NR	EEG segments of recording	EEG filters, amplitude and duration criteria and treatment of artifacts

[a]Citation number in References of this paper.
[b]Authors.
[c]Sensitivity, specificity, and FP rate: same as Table I; NR: information not reported.
[d]Total recordings: Total number of recordings in study.
[e]Subjects: Age distribution, categorized as adults, children, or infants. All studies in this list work with healthy subjects.
[f]Datasets: Distribution and length of recordings in datasets; NR: information not reported.
[g]Sample universe: Type of recordings and number of SS events marked by sleep experts.
[h]Methodology: Main tools used in each study.

TABLE IV
COMPARISON OF DIFFERENT PUBLISHED AUTOMATED SS DETECTION SYSTEMS: RESULTS FOR NREMS-2 SEGMENTS

Ref.[1]	Authors[2]	SS detection in NREMS-2			Total recordings[4]	Subjects[5]	Data sets[6]	Sample Universe[7]	Methodology[8]
		Sensitivity[3] [%]	Specificity[3] [%]	False-positive rate[3] [%]					
	This work	92.2	90.1	8.9	56	Children	Training: 26 rec. Validation: 10 rec. Testing: 19 rec.	Complete all-night sleep recording. 40,412 SS events on testing set	EMD-HHT, FFT, fuzzy logic, features extraction and expert's procedure
[26]	Huupponen et al. (2007)	70.0	98.6	32.0	12	Adults	Training and testing data sets are the same	Complete all-night sleep recording. 6,043 SS events on testing data set	FFT, EEG filters, amplitude analysis and fuzzy detectors
[29]	Ventouras et al. (2005)	83.4	92.9	9.7	1	Adult	Training and testing data set are the same	3 EEG segments of recording in NREMS-2. 182 SS events on testing data set	Multi-layer perceptron (MLP) architecture
[30]	Gorur et al. (2002)	88.7	NR	NR	NR	Adults	Training: 1,000 SS & non-SS samples. Testing: 1,142 SS & non-SS samples	EEG segments in NREMS-2	Feature extraction and MLP
[30]	Gorur et al. (2002)	95.4	NR	NR	NR	Adults	Training: 1,575 SS & non-SS samples. Testing: 175 SS & non-SS samples	EEG segments in NREMS-2	Feature extraction and suport vector machine (SVM)
[32]	Zygierewicz et al. (1999)	90.0	NR	NR	10	Adults	NR	EEG segments in NREMS-2	Feature extraction, matching pursuit and amplitude criteria

their results fall below our ROC curve. For the continuous all-night recordings, the results obtained by Bódizs *et al.* [25] fall close to our curve, with a performance similar to the output of Module 3. A wider comparison with other SS detection systems described in the literature and mentioned in the introduction is shown in Tables III and IV.

Comparing the databases used by the different research groups, our database seems to be the largest, with a total of 56 all-night sleep recordings. The same holds true for the number of SS events marked by the experts, as we have a total of 111 524 SS events. Regarding the type of data, only Huupponen *et al.* [26], [27] and our work use all-night sleep recordings; other

groups use segments of EEG recordings [25], [28]–[32], [34]. On the other hand, our group is one of the few that focuses on automated detection in infants and children recordings [28], [33], [39], [40], [54]. Most studies apply their work on adults sleep recordings [25]–[27], [29]–[32], [34], [55], [56].

V. Discussion and Conclusion

We developed a new method to detect and characterize SS events in continuous all-night sleep recordings, based on advanced signal processing tools as FFT, EMD, HHT, fuzzy logic, and feature extraction. FFT provides the capacity to search for EEG zones compatible with the presence of SS events without requiring a hypnogram. This is relevant because the hypnogram creation is a time-consuming task for the sleep experts. EMD and HHT allow for discriminating SS trains in the time and frequency domains, generating enhanced temporal location of SS events throughout the EEG recording, preventing under- and overestimation of the duration of the SS events detected. In addition, fuzzy logic and feature extraction allow to emulate the expert's procedure during visual inspection.

The proposed method shows an expert-system agreement (sensitivity) for continuous all-night sleep recordings of 88.2%, and considering only NREMS-2, this performance is 92.2%. These results fall in the upper limit of the study by Campbell *et al.* [23] about human and automatic SS detection that show an expert–system agreement of 80%–90%.

This study has limitations, which need to be considered. With a bipolar montage, fronto-to-central derivations for this study, we could not evaluate the precise location of SS waves. For instance, frontal and central SS appear to follow somewhat different developmental paths, with the first being slower in the same individual [57], [58], thus suggesting the existence of different generators or a topographical difference during maturation of the thalamocortical network [57], [58]. It seems possible that analyzing frontal and central derivations independently, rather in combined derivations, might provide even better results. The same holds true for other known modifiers of SS characteristics, like sleep restriction or deprivation, circadian phase, or pharmacologic effects [59]. Because our recordings were performed in healthy subjects during their naturally occurring sleep–wake cycle without affecting the usual routine, we were unable to evaluate the influence of these upon SS features. Since the aforementioned factors might help to strengthen our results, they could be the focus for future studies.

The reliance of our system on several thresholds selected empirically may reduce the application by other laboratories. The replication of a process like the one we used (training/validation/testing) should help to clarify its applicability for other groups. On the other hand, we believe that it also provides a challenge for the field to consider more innovative approaches to identify sleep patterns and SS in particular. This could be even more relevant when considering the few published studies that have compared visual and automated scorings of polysomnographic data in infancy and childhood, as it was recently reported by the Pediatric Task Force and the Scoring Manual Steering Committee of the American Academy of Sleep Medicine [5].

The construction of a large 56 all-night children polysomnographic database, which can be used to train and test this and other methods, is among the important achievements of this paper, and it certainly contributes to its robustness. It is among the most complete and largest annotated databases of this type in children.

References

[1] M. Steriade, "Grouping of brain rhythms in corticothalamic systems," *Neuroscience*, vol. 137, no. 4, pp. 1087–1106, 2006.

[2] R. W. McCarley, "Neurobiology of REM and NREM sleep," *Sleep Med.*, vol. 8, no. 4, pp. 302–330, 2007.

[3] A. Rechtschaffen and A. Kales, "A manual of standardized terminology, techniques and scoring system for sleep stages of human subjects," presented at the UCLA, Brain Research Institute/Brain Information Service, Los Angeles, CA, 1968.

[4] M. H. Bonnet, K. Doghramji, T. Roehrs, E. J. Stepanski, S. H. Sheldon, A. S. Walters, M. Wise, and A. L. Chesson, "The scoring of arousal in sleep: Reliability, validity, and alternatives," *J. Clin. Sleep Med.*, vol. 3, no. 2, pp. 133–145, 2007.

[5] M. Grigg-Damberger, D. Gozal, C. L. Marcus, S. F. Quan, C. L. Rosen, R. D. Chervin, M. Wise, D. L. Picchietti, S. H. Sheldon, and C. Iber, "The visual scoring of sleep and arousal in infants and children," *J. Clin. Sleep Med.*, vol. 3, no. 2, pp. 201–240, 2007.

[6] M. H. Silber, S. Ancoli-Israel, M. H. Bonnet, S. Chokroverty, M. M. Grigg-Damberger, M. Hirshkowitz, S. Kapen, S. A. Keenan, M. H. Kryger, T. Penzel, M. R. Pressman, and C. Iber, "The visual scoring of sleep in adults," *J. Clin. Sleep Med.*, vol. 3, no. 2, pp. 121–131, 2007.

[7] P. Peirano and C. Algarín, "Sleep in brain development," *Biol. Res.*, vol. 40, no. 4, pp. 471–478, 2007.

[8] M. P. Walker, T. Brakefield, A. Morgan, A. J. Hobson, and R. Stickgold, "Practice with sleep makes perfect: Sleep-dependent motor skill learning," *Neuron*, vol. 35, no. 1, pp. 205–211, 2002.

[9] M. P. Walker and R. Stickgold, "Sleep, memory, and plasticity," *Annu. Rev. Psychol.*, vol. 57, no. 1, pp. 139–166, 2006.

[10] S. S. Yoo, P. T. Hu, N. Gujar, F. A. Jolesz, and M. P. Walker, "A deficit in the ability to form new human memories without sleep," *Nat. Neurosci.*, vol. 10, no. 3, pp. 385–392, 2007.

[11] P. Peirano, C. Algarín, M. Garrido, D. Algarín, and B. Lozoff, "Iron-deficiency anemia is associated with altered characteristics of sleep spindles in NREM sleep in infancy," *Neurochem. Res.*, vol. 32, no. 10, pp. 1665–1672, 2007.

[12] M. Rosanova and D. Ulrich, "Pattern-specific associative long-term potentiation induced by a sleep spindle-related spike train," *J. Neurosci.*, vol. 25, no. 41, pp. 9398–9405, 2005.

[13] M. Steriade, "Coherent oscillations and short-term plasticity in corticothalamic networks," *Trends Neurosci.*, vol. 22, no. 8, pp. 337–345, 1999.

[14] M. Steriade and F. Amzica, "Coalescence of sleep rhythms and their chronology in corticothalamic networks," *Sleep Res. Online*, vol. 1, no. 1, pp. 1–10, 1998.

[15] M. Schabus, G. Gruber, S. Parapatics, C. Sauter, G. Klösch, P. Anderer, W. Klimesch, B. Saletu, and J. Zeitlhofer, "Sleep spindles and their significance for declarative memory consolidation," *Sleep*, vol. 27, no. 8, pp. 1479–1485, 2004.

[16] M. Schabus, K. Hödlmoser, G. Gruber, C. Sauter, P. Anderer, G. Klösch, S. Parapatics, B. Saletu, W. Klimesch, and J. Zeitlhofer, "Sleep spindle-related activity in the human EEG and its relation to general cognitive and learning abilities," *Eur. J. Neurosci.*, vol. 23, no. 7, pp. 1738–1746, 2006.

[17] C. Smith and C. MacNeill, "Impaired motor memory for a pursuit rotor task following stage 2 sleep loss in college students," *J. Sleep Res.*, vol. 3, no. 4, pp. 206–213, 1994.

[18] M. P. Walker, "The role of sleep in cognition and emotion," *Ann. NY. Acad. Sci.*, vol. 1156, no. 1, pp. 168–197, 2009.

[19] M. Schabus, K. Hödlmoser, T. Pecherstorfer, P. Anderer, G. Gruber, S. Parapatics, C. Sauter, G. Kloesch, W. Klimesch, B. Saletu, and J. Zeitlhofer, "Interindividual sleep spindle differences and their relation to learning-related enhancements," *Brain Res.*, vol. 1191, pp. 127–135, 2008.

[20] M. Tamaki, T. Matsuoka, H. Nittono, and T. Hori, "Activation of fast sleep spindles at the premotor cortex and parietal areas contributes to motor learning: A study using sLORETA," *Clin. Neurophysiol.*, vol. 120, no. 5, pp. 878–886, 2009.

[21] M. Tamaki, T. Matsuoka, H. Nittono, and T. Hori, "Fast sleep spindle (13-15 hz) activity correlates with sleep-dependent improvement in visuomotor performance," *Sleep*, vol. 31, pp. 204–211, 2008.
[22] H. A. Parmelee, M. Sigman, J. Garbanati, S. Cohen, L. Beckwith, and R. Asarnow, "Neonatal electroencephalographic organization and attention in early adolescence," in *Human Behavior and the Developing Brain*, G. Dawson and K. Fischer, Eds. New York: Guilford, 1994, pp. 537–554.
[23] K. Campbell, A. Kumar, and W. Hofmann, "Human and automatic validation of a phase-locked loop spindle detection system," *Electroencephalogr. Clin. Neurophysiol.*, vol. 48, no. 5, pp. 602–605, 1980.
[24] D. Kunz, H. Danker-Hopfe, G. Gruber, J. L. Lorenzo, S. L. Himanen, B. Kemp, T. Penzel, J. Röschke, and G. Dorffner, "Interrater reliability between eight European sleep-labs in healthy subjects of all age-groups," *J. Sleep Res.*, vol. 9, supp. 1, p. 106, 2000.
[25] R. Bódizs, J. Körmendi, P. Rigó, and A. Sándor Lázár, "The individual adjustment method of sleep spindle analysis: Methodological improvements and roots in the fingerprint paradigm," *J. Neurosci. Meth.*, vol. 178, no. 1, pp. 205–213, 2009.
[26] E. Huupponen, G. Gómez-Herrero, A. Saastamoinen, A. Värri, J. Hasan, and S. Himanen, "Development and comparison of four sleep spindle detection methods," *Artif. Intell. Med.*, vol. 40, no. 3, pp. 157–170, 2007.
[27] E. Huupponen, A. Värri, S.-L. Himanen, J. Hasan, M. Lehtokangas, and J. Saarinen, "Optimization of sigma amplitude threshold in sleep spindle detection," *J. Sleep Res.*, vol. 9, pp. 327–334, 2000.
[28] P. A. Estévez, R. Zilleruelo-Ramos, R. Hernández, L. Causa, and C. M. Held, "Sleep spindle detection by using merge neural gas," presented at the 6th Int. WSOM, Bielefeld, Germany, 2007.
[29] E. M. Ventouras, E. A. Monoyiou, P. Y. Ktonas, T. Paparrigopoulos, D. G. Dikeos, N. K. Uzunoglu, and C. R. Soldatos, "Sleep spindle detection using artificial neural networks trained with filtered time-domain EEG: A feasibility study," *Comput. Meth. Prog. Bio.*, vol. 78, no. 3, pp. 191–207, 2005.
[30] D. Gorur, U. Halici, H. Aydin, G. Ongun, F. Ozgen, and K. Leblebicioglu, "Sleep-spindles detection using short time Fourier transform and neural networks," in *Proc. IEEE IJCNN*, Honolulu, HI, May 12–17, 2002, vol. 2, pp. 1631–1636.
[31] S. V. Schönwald, E. L. de Santa-Helena, R. Rossatto, M. L. Chaves, and G. J. Gerhardt, "Benchmarking matching pursuit to find sleep spindles," *J. Neurosci. Meth.*, vol. 156, no. 1–2, pp. 314–321, 2006.
[32] J. Zygierewicz, K. J. Blinowska, P. J. Durka, W. Szelenberger, S. Niemcewicz, and W. Androsiuk, "High resolution study of sleep spindles," *Clin. Neurophysiol.*, vol. 110, no. 12, pp. 2136–2147, 1999.
[33] C. M. Held, L. Causa, P. Estévez, C. Pérez, M. Garrido, C. Algarín, and P. Peirano, "Dual approach for automated sleep spindles detection within EEG background activity in infant polysomnograms," in *Proc. 26th IEEE IEMBS*, San Francisco, CA, Sep. 1–5, 2004, vol. 1, pp. 566–569.
[34] P. Schimicek, J. Zeitlhofer, P. Anderer, and B. Saletu, "Automatic sleep-spindle detection procedure: Aspects of reliability and validity," *Clin. Electroencephal.*, vol. 25, no. 1, pp. 26–29, 1994.
[35] G. Rilling, P. Flandrin, and P. Gonçalves, "On empirical mode decomposition and its algorithms," presented at the IEEE-EURASIP NSIP, vol. 1, Italy, 2003.
[36] N. E. Huang, Z. Shen, S. R. Long, M. C. Wu, H. H. Shih, Q. Zheng, N. C. Yen, C. C. Tung, and H. H. Liu, "The empirical mode decomposition and the Hilbert spectrum for nonlinear and non-stationary time series analysis," in *Proc. Roy. Soc. Lond.*, 1998, vol. A 454, no. 1971, pp. 903–995.
[37] H. H. Jasper, "The ten-twenty electrode system of the international federation," *Electroencephalogr. Clin. Neurophysiol.*, vol. 10, pp. 371–375, 1958.
[38] B. Kemp, A. Värri, A. C. Rosa, K. D. Nielsen, and J. Gade, "A simple format for exchange of digitized polygraphic recordings," *Electroencephalogr. Clin. Neurophysiol.*, vol. 82, no. 5, pp. 391–393, 1992.
[39] P. A. Estévez, C. M. Held, C. A. Holzmann, C. A. Perez, J. P. Pérez, J. Heiss, M. Garrido, and P. Peirano, "Polysomnographic pattern recognition for automated classification of sleep-waking states in infants," *Med. Biol. Eng. Comput.*, vol. 40, pp. 105–113, 2002.
[40] J. E. Heiss, C. M. Held, P. A. Estévez, C. A. Perez, C. A. Holzmann, and J. P. Pérez, "Classification of sleep stages in infants: A neuro fuzzy approach," *IEEE Eng. Med. Biol. Mag.*, vol. 21, no. 5, pp. 147–151, Sep./Oct. 2002.
[41] M. Jobert, E. Poiseau, P. Jahnig, H. Schulz, and S. Kubicki, "Topographical analysis of sleep spindle activity," *Neuropsychobiology*, vol. 26, no. 4, pp. 210–217, 1992.
[42] E. Werth, P. Achermann, D. Dijk, and A. Borbély, "Spindle frequency activity in the sleep EEG: Individual differences and topographical distribution," *Electroencephalogr. Clin. Neurophysiol.*, vol. 103, no. 5, pp. 535–542, 1997.
[43] J. Zeitlhofer, G. Gruber, P. Anderer, S. Asenbaum, P. Schimicek, and B. Saletu, "Topographic distribution of sleep spindles in young healthy subjects," *J. Sleep Res.*, vol. 6, no. 3, pp. 149–155, 1997.
[44] P. A. Estévez and C. J. Figueroa, "Online data visualization using the neural gas network," *Neural Netw.*, vol. 19, no. 6/7, pp. 923–934, 2006.
[45] T. M. Martinetz and J. Schulten, "A neural-gas network learns topologies," in *Artificial Neural Networks*, T. Kohonen, K. Mäkisara, O. Simula, and J. Kangas, Eds. Amsterdam: North-Holland, 1991, pp. 397–402.
[46] S. Haykin, *Neural Networks: A Comprehensive Foundation*. New York, NY: Macmillan College Publishing, 1994.
[47] T. Kohonen Ed., *Self-Organizing Maps* (Series in Information Sciences), vol. 30, 3rd ed. Berlin, Germany: Springer, 2001.
[48] R. S. Horne, C. Egodagamage, S. M. Cranage, and T. M. Adamson, "Effect of infant sleeping position on sleep spindles," *J. Sleep Res.*, vol. 12, no. 1, pp. 19–24, 2003.
[49] S. Gais, M. Mölle, K. Helms, and J. Born, "Learning-dependent increases in sleep spindle density," *J. Neurosci.*, vol. 22, no. 15, pp. 6830–6834, 2002.
[50] H. Liang, S. Bressler, R. Desimone, and P. Fries, "Empirical mode decomposition: A method for analyzing neural data," *Neurocomputing*, vol. 65/66, pp. 801–807, 2005.
[51] A. O. Andrade, S. Nasuto, P. Kyberd, C. M. Sweeney-Reed, and F. R. Van Kanijn, "EMG signal filtering based on empirical mode decomposition," *Biomed. Signal Process. Control*, vol. 1, no. 1, pp. 44–55, 2006.
[52] R. Fonseca-Pinto, J. L. Ducla-Soares, F. Araújo, P. Aguiar, and A. Andrade, "On the influence of time-series length in EMD to extract frequency content: Simulations and models in biomedical signals," *Med. Eng. Phys.*, vol. 31, no. 6, pp. 713–719, 2009.
[53] J.-R. Yeh, S.-Z. Fan, and J.-S. Shieh, "Human heart beat analysis using a modified algorithm of detrended fluctuation analysis based on empirical mode decomposition," *Med. Eng. Phys.*, vol. 31, no. 1, pp. 92–100, 2009.
[54] C. M. Held, J. E. Heiss, P. A. Estévez, C. A. Perez, M. Garrido, C. Algarín, and P. Peirano, "Extracting fuzzy rules from polysomnographic recordings for infant sleep classification," *IEEE Trans. Biomed. Eng.*, vol. 53, no. 10, pp. 1954–1962, Oct. 2006.
[55] R. Agarwal and J. Gotman, "Computer-assisted sleep staging," *IEEE Trans. Biomed. Eng.*, vol. 48, no. 12, pp. 1412–1423, Dec. 2001.
[56] J. C. Principe, S. K. Gala, and T. G. Chang, "Sleep staging automaton based on the theory of evidence," *IEEE Trans. Biomed. Eng.*, vol. BME-36, no. 5, pp. 503–509, May 1989.
[57] F. A. Gibbs and E. L. Gibbs, *Atlas of Electroencephalography,* vol. 1. Reading, MA: Addison-Wesley, 1950.
[58] S. Shinomiya, K Nagata, K. Takahashi, T. Masumura, "Development of sleep spindles in young children and adolescents," *Clin. Electroencephalogr.*, vol. 30, pp. 39–43, 1999.
[59] L. De Gennaro and M. Ferrara, "Sleep spindles: An overview," *Sleep Med. Rev.*, vol. 7, pp. 423–440, 2003.

Leonardo Causa received the B.S. degree in electrical engineering (EE) from the Universidad de Chile (U. de Chile), Santiago, Chile, in 2003, where he is currently working toward the P.E. (EE) degree in civil engineering, and the M.S. degree in biomedical engineering (BME), he is also working toward the Ph.D. degree in BME by cotutelage from U. de Chile and Université Claude Bernard Lyon 1, Lyon, France.

His research interests include sleep pattern recognition, signal and image processing, neurofuzzy systems applied to the classification of physiological data. He was engaged in research on fraud detection in long-distance telecommunications, automated sleep-pattern detection and respiratory signal analysis.

Claudio M. Held (M'91–SM'08) received the B.S. degree in electrical engineering (EE), the degree in electrical civil engineering, and the M.S. degree in biomedical engineering (BME) from the Universidad de Chile (U. de Chile), Santiago, Chile, in 1990, and the Ph.D. degree in BME from Rensselaer Polytechnic Institute, Troy, NY, in 1995.

He is currently an Adjunct Professor of EE at U. de Chile, where he is also the Head of the sleep signals research group in the EE Department. He is also a Managing Director at Apacomint Ltda, Santiago. His research interests include applying fuzzy logic and intelligent systems in BME and other areas of decision making. He was engaged in research on automated EKG interpretation, multiple drug infusion, classification of sleep-waking states in infants, handwritten digit recognition, fraud detection in long-distance telecommunications, health insurance pricing, face identification, online trucks diagnostics, etc.

Javier Causa received the B.S. degree in electrical engineering (EE) from the Universidad de Chile, Santiago, Chile, in 2006, where he is currently working toward the P.E. degree in electrical civil engineering and the M.S. degree in EE.

His current research interests include sleep patterns recognition and neurofuzzy systems applied to the classification of physiological data. He was engaged in research on automated sleep-pattern detection and online trucks diagnostics.

Pablo A. Estévez (M'98–SM'04) received the B.S. degree and the P.E. degree in electrical engineering (EE) from the Universidad de Chile (U. de Chile), Santiago, Chile, in 1978 and 1981, respectively, and the M.Eng. and Dr.Eng. degrees from the University of Tokyo, Tokyo, Japan, in 1992 and 1995, respectively.

He is currently the Chairman and an Associate Professor of the EE Department, U. de Chile. He was an Invited Researcher at the NTT Communication Science Laboratory, Kyoto, Japan, the Ecole Normale Supérieure, Lyon, France, and a Visiting Professor at the University of Tokyo, Tokyo, Japan.

Dr. Estévez is a distinguished Lecturer of the IEEE Computational Intelligence Society (CIS) and a member-at-large of the IEEE CIS ADCOM. He is an Associate Editor of the IEEE TRANSACTIONS ON NEURAL NETWORKS.

Claudio A. Perez (M'92–SM'04) received the B.S. and P.E. degrees in electrical engineering (EE) and the M.S. degree in biomedical engineering from the Universidad de Chile (U. de Chile), Santiago, Chile, in 1980 and 1985, respectively, and the Ph.D. degree from Ohio State University (OSU), Columbus, in 1991.

He was a Fulbright student at Ohio State University. In 2002, he was a Visiting Scholar at University of California, Berkeley through the Alumni Initiatives Award Program from Fulbright Foundation. He is currently a faculty member in the Department of EE, U. de Chile, where he was the Chairman from 2003 to 2006. He is a member of the Editorial Board of the *International Journal of Optomechatronics* and an Associate Editor of the *Biomedical Engineering-Neuroscience*. His research interests include man–machine interfaces, biometrics, and pattern recognition.

Dr. Perez is a Senior Member of the IEEE SYSTEMS, MAN, AND CYBERNETICS, the IEEE Computational Intelligence Society, the Sigma-Xi, and the OSU Alumni Association.

Rodrigo Chamorro received the Nutritionist degree from the Universidad de Concepción, Chile, in 2004, and the M.S. degree in human nutrition from the Universidad de Chile (U. de Chile), Santiago, Chile, in 2008, where he is currently working toward the Ph.D. degree in nutrition and food.

Since 2006, he has been at the Sleep Laboratory at the Instituto de Nutrición y Tecnología de los Alimentos, U. de Chile. His current research interests include the role of sleep and endocrine patterns on the development of obesity and related diseases.

Marcelo Garrido received the M.S. degree from the Universidad de Chile (U. de Chile), Santiago, Chile.

He is currently an Associate Researcher at the Sleep Laboratory, Instituto de Nutrición y Tecnología de los Alimentos, U. de Chile. His research interests include the study of motor activity and heart rate patterns during the sleep–wake cycle in early human development.

Cecilia Algarín received the M.D. degree from Universidad Javeriana, Colombia, in 1981, and specialized in pediatric neurology in 1987.

She was in the Hospital Universitario, Barranquilla, Colombia, until 1994. During 1995 and 1996, she was a Fellow in neuroradiology at Emory University, Atlanta, GA. Since 1997, she has been at the Sleep and Neurobiology Laboratory, Instituto de Nutrición y Tecnología de los Alimentos, Universidad de Chile, Santiago, Chile, where she has been a Researcher and an adjunct Professor, Instituto de Nutrición y Tecnología de los Alimentos, U. de Chile. She was engaged in several projects funded by the National Institutes of Health and Fondo Nacional de Desarrollo Científico y Tecnológico (Chile), as well collaborated with the Center for Human Development, University of Michigan, Ann Arbor, Laboratory for Neurocognitive Development, Pittsburgh University, Pittsburgh, PN, Laboratories of Cognitive Neuroscience, Harvard Medical School, Boston, MA, and Institute for Research of Mental Retardation and Cerebral Aging (OASI), Troina, Italy.

Patricio Peirano received the M.D. degree from the Universidad de Chile (U. de Chile), Santiago, Chile, in 1980, and the Ph.D. degree from the University of Paris, France, in 1989, and completed training in neurophysiology and sleep medicine.

In 1990, he was the Founder of the Sleep and Functional Neurobiology Laboratory, Instituto de Nutrición y Tecnología de los Alimentos, U. de Chile, where he is currently a Full Professor of neurophysiology and sleep medicine and also the Head of the laboratory.